

Numerical and experimental full synchronization of 2×2 optoelectronic device network

Farah Farman^{a,*}, Hind A. Jasim^a, Ahmed Sameer^a, Asmaa Abdulrahman Haneen^a

^aAl-Esraa University College, Iraq

(Communicated by Madjid Eshaghi Gordji)

Abstract

Numerically and experimentally the full synchronization of 2×2 optoelectronic device network. By the using of 2×2 oscillator's network, every one of the oscillators has been considered as optocoupler (i.e. LED that has been coupled with photodetector). By fixing the strength of the feedback (\mathcal{E}) and increasing the current of the bias (δ) of every one of the oscillators, the dynamic sequence like chaotic and periodic mixed-mode oscillations has been observed. Synchronization of unidirectionally coupled optoelectronic devices network has been featured when bias current equal to 4.4×10^{-4} . Transitions between the synchronization and the non-synchronization states through spatiotemporal distributions have been investigated.

Keywords: LED, chaos, feedback, synchronization

1. Introduction

Chaos synchronization was utilized to the systems of communication over a wide bandwidth range in the last 10 years [14, 10]. Physics, chemistry, engineering, weather and climate, and even economics [9] are all examples chaos. This study provided an approach for synchronizing 2 chaotic systems that are identical but have distinct initial circumstances. In laser physics, secure communication, chemical reactors, biomedicine, and other fields, chaos synchronization has various uses. The active control approach, linear feedback method, time-delay feed-back method, adaptive technique, and back stepping approach are only a few of the chaotic control and synchronization strategies that were created [21, 22]. The discovery by Carroll and Pecorra [14] of the potential of synchronizing chaotic

*Corresponding author

Email addresses: farah.farman@esraa.edu.iq (Farah Farman), hind.ahmed@esraa.edu.iq (Hind A. Jasim), noor.mohammed@esraa.edu.iq (Noor Mohammed Ibrahim), asma.hanen@esraa.edu.iq (Asmaa Abdulrahman Haneen)

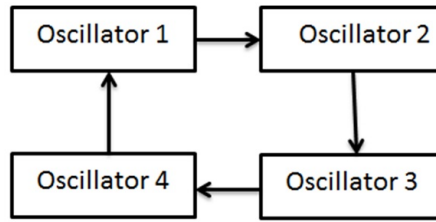


Figure 1: The configuration of the nearest neighbor closed loop.

transmitter and receiver resulted in the application of chaos for secure communication in optical and electrical domains. The finding of synchronized chaos is considered as one of the major intriguing recent advances in non-linear dynamics. Yamada and Fujisaka [4, 23] and Carroll and Pecora [14] were the first to report the potential of synchronization in a connected chaotic system constituted of the similar chaotic oscillators. Generalized synchronizations [20], complete synchronizations [8, 16], lag synchronization [17], phase synchronization [6], projective synchronizations [7], ant synchronization [12, 5] are some examples of synchronization regimes. The systems could be different or identical, with bidirectional (mutual coupling) or unidirectional (drive–response or master–slave coupling) coupling and stochastic or deterministic driving forces [19]. Nd: YAG [18] and CO₂ lasers [11] have been used in the 1st experimental demonstrations regarding the synchronization of 2 chaotic lasers in lasers’ field. Also, the theoretical study of the synchronizations in a network of coupled LED in the existence of AC-filtered non-linear opto-electronic feedback [1]. In the MMOs regime [3], a chaotic oscillator depending on incoherent light sources (LEDs) with AC coupling can be used to build a four-element network. This study showed full synchronization between LEDs as a network both experimentally and theoretically. LEDs are coupled in a uni-direction.

2. Dynamical Model

Figure 1 depicts the configuration, which consists of 4 oscillators, each of which is an optocoupler (LED coupled with photo-detector) with non-linear AC coupled optoelectronic feedback. Also, the transistor photocurrent couples such oscillators, creating a network in the nearest neighbor configuration.

The most straightforward method is modelling LED as a p-n junction, 3 coupled variables, carrier (i.e. electron) density (N), high-pass-filtered feedback voltage (V_f), and the junction applied voltage (V_d), all of which evolve on very distinct time scales, dictate the system dynamics. The carrier density is expected to be proportional to the light intensity (N) [2].

$$\dot{N} = -\gamma_{SP}\dot{N} + \frac{MN(V_b - V_{bi})}{\Delta^2} \quad (2.1)$$

$$C\dot{V}_d = \frac{V_o - V_d + F_f(V_f)}{R} - \frac{e\mu NS(V_d - V_{bi})}{\Delta} \quad (2.2)$$

$$\dot{V}_f = -\gamma V_f + \dot{K}\varphi \quad (2.3)$$

In which (γ_{SP}) represents the rate of the spontaneous emission, (μ) represents the mobility of the carrier, (C) represents the capacitance of the diode (i.e. the voltage that is independent for the simplicity), (R) represents current-limiting resistor, (V_0) represents dc bias voltage, (e) represents the charge of the electron, $F_f(V_f)$ represents the function of the feedback amplifier, (k) represents

photodetector responsively, and (φ) represents density of photon, linearly proportional to carrier density $\dot{\mathcal{O}} = \eta N$, in which (η) represents LED quantum efficiency. Eq (2.1). specifies that there is a decrease in the (N) in active layer because of the radiative re-combination and increased with the forward injection current density $J = [e\mu N(V_b - V_{bi})]/\Delta$. In addition, non-radiative recombination as well as carrier generation through optical absorption were neglected because they don't considerably change dynamics. Equation (2.2) represents the Kirchhoff law regarding a circuit (i.e. the resistors-ideal diode) which relates the voltage of the junction (V_d) with dc applied voltage V_o [2nd term] in Eq.(2.2) represents the flow of the current across diode $[I = JS]$. Eq(2.3) indicates a non-linear feedback loop, in which the signal of the voltage which comes from a detector $(k\phi)$ has been high-pass filtered as well as added to dc bias via a function of the amplifier $F_f(V_f)$. Considering only solitary LED eqs. (2.1) and (2.2). Furthermore, a finite stationary carrier density, which linearly increased with (V_0) , has been identified just when $V_d > V_{th} \equiv V_{bi} + \gamma sp \Delta 2/\mu$; otherwise, the only stationary solution is $N = 0$ and $V_d = V_0$ (0current). Therefore, the emission of the light starts in the case where the voltage that has been applied (V_o) is exceeding the voltage of the threshold (V_{th}) . Through presenting dimension-less variable $x = e\mu RS N/\Delta$, $y = \mu(V_d - V_{bi})/\Delta 2\gamma sp$, and $w = \frac{e\mu RS}{k\eta\Delta} V_f - x$ and the time scalet' = γspt .

$$\frac{dx}{dt} = X1(Y1 - 1) + \delta Y1 \tag{2.4}$$

$$\frac{dy}{dt} = \frac{-\gamma(-\delta + y1 - a(x1 + z1))}{(1 + s(x1 + z1)) + x1y1} \tag{2.5}$$

$$\frac{dz}{dt} = -e(z + x1) \tag{2.6}$$

where $f(z + x) \equiv \alpha(z + x)/(1 + s(z + x))$, $\delta 0 = (V_0 - V_{bi})/(V_{th} - V_{bi})$, $\varepsilon = \gamma f/\gamma sp$, $\alpha\gamma = 1/RC\gamma sp$ $s = k\eta\Delta s/e\mu RS$,

In such a case, y and x represent appropriately normalized photon and population-inversion density values, respectively, and (γ) represents photon-to-carrier lifetime ratio. In [3, 13], the dynamical process underlying MMOs in the system was thoroughly examined. In the case when employing Berkeley Madonna (BM) software, the results should be simple to handle. The non-linear dynamics related to LED with OEFD are demonstrated by equations ((2.4), (2.5) and (2.6)). Also, the 1st eq. represents photon density or output diode intensity. The symbol for the inversion of the populations is the second eq., while the feedback symbol that is required to generate chaos is the third equation. For analytical and numerical purposes, N-LED system can be represented in dimensionless [15]:

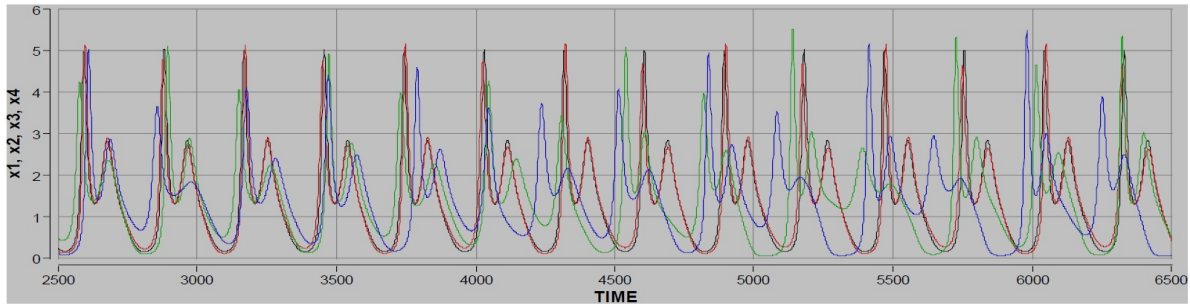
$$\dot{x}_i = x_i(y_i - 1) + \gamma y_i \tag{2.7}$$

$$\dot{y}_i = \gamma(\delta - y_i + \frac{a(z_i + x_i)}{(1 + s(z_i + x_i))} - x_i y_i) \tag{2.8}$$

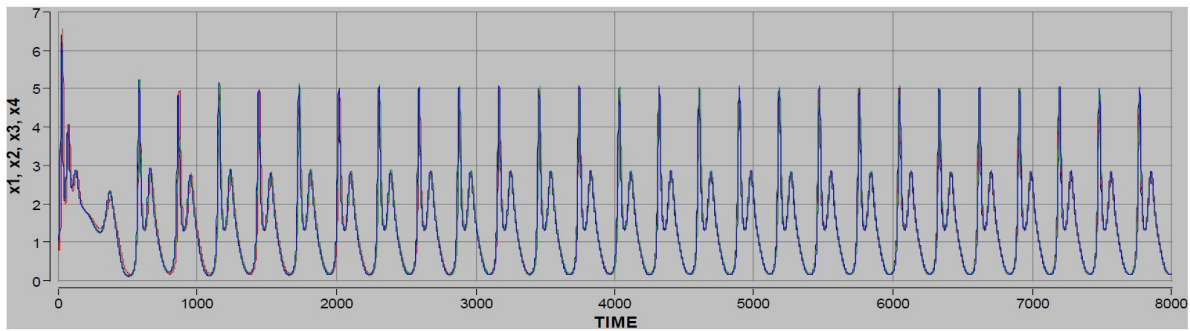
$$\dot{z}_i = -\varepsilon(z_i + x_i) + \sum_{j=1}^N g_{ij} z_j \tag{2.9}$$

$$i = 1, 2, \dots, N$$

In which y - carrier density, x denotes photon density, z denotes high-pass filter feed-back current, where δ represents the threshold current of the solitary laser, γ represents ratio of carrier to photon



(a)



(b)

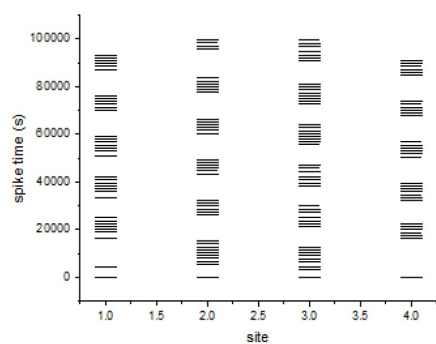
Figure 2: (a) non-synchronization amongst four oscillators. (b) full-synchronization of four oscillators.

life-times, a term $a \frac{(x+z)}{(1+s(z+x))}$ indicates the function of the feed-back amplifier, in which a represents the gain of the amplifier and s represents a coefficient of saturation, g_{ij} represents the strength of the coupling. The parameters of the system have been set to $a = 1$, $\gamma = 0.01$, $s = 0.2$, $N = 4$, and $\delta = 2.75$.

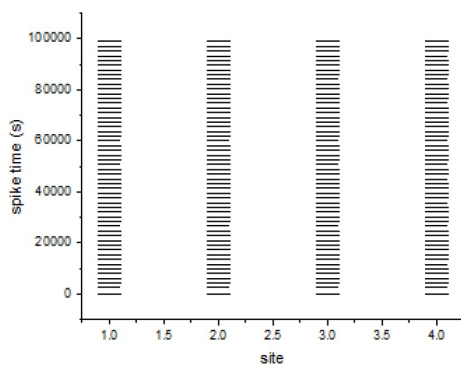
3. Numerical Results

In the case when employing Berkeley Madonna (BM) software with the Origin Lab tool, the findings should be simple to handle. The feed-back strength and bias have been utilized for feeding all oscillators in such situation because 4 LEDs were coupled. Figure 3 shows the dynamical sequence in which the strength of the feedback (\mathcal{E}) is fixed and bias current (δ) grows in each oscillator. Figure 2a shows non-synchronization; as the g value gradually increases, the spiking occurs in an identical time series; at a value of $g = 4.4 E - 4$, full synchronization regarding periodic mix-mode oscillation is achieved, as it has been illustrated in Fig.2b.

In the system, the order degree has been identified with its spatio-temporal distribution in order to quantify the rapid change. Figure 3a indicates that in the case where the factor of the coupling g equals 0, oscillators run in an independent manner (i.e. non-synchronization), and spikes have a distribution of various times. The synchronization appearance indicates that perturbation from 1st oscillator has propagated through network, with entire array that reaches last oscillator and every peak having equal time distributions, which has been illustrated by Fig.3b.



(a)



(b)

Figure 3: Spatiotemporal distribution of the numerical results (a) conditions of non-synchronization. (b) Fully-synchronized.

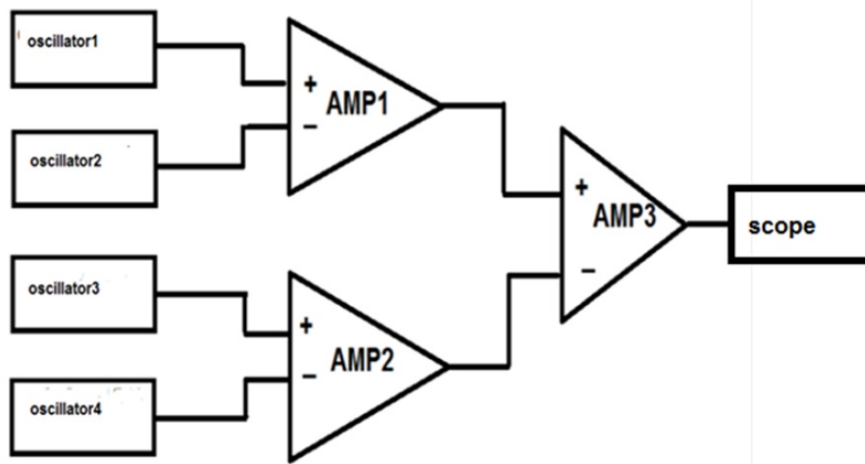


Figure 4: Diagram of experimental setup for the synchronization.

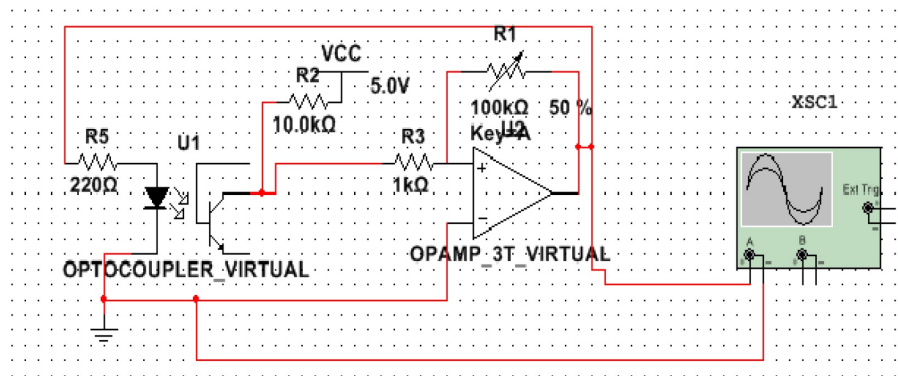


Figure 5: Oscillator (i.e. opto-coupler and operation amplifier).

4. Experimental Part

In the case where small signal gain of the amplifier is feed-back to LED and supplemented by DC current bias, an appropriate signal level to generate the mixed mode oscillations dynamics has been obtained. In order to explore synchronization between optoelectronic devices, a network of them must be created. As illustrated in Figure 4, this study examines the experimental treatment regarding the chaos synchronization in a network system. Also, the network is made up of 4 oscillators, each of which includes an optocoupler and an operational amplifier (op-amp). As indicated in Figure 5, the oscillator is made up of an (op-amp) and an optocoupler. The signal of the output is sent to the amplifier of the variable gain op. which is identified by non-linear transfer function of a following representation:

$$f(w) = Aw/(1 + sw)$$

In which A represents gain of the amplifier and s the coefficient of saturation, and after that feed-back to LED injection current.

The 3rd differential amplifier receives the outputs of AMP (1) and (2). Through playing LED DC bias current of all, the output regarding such differential amplifier (3) was regulated to the digital oscilloscope. One might attain the synchronization condition in the case when every one of the LEDs has been independent and opto-electronic feed-back of all of the differential amplifiers has been fixed.

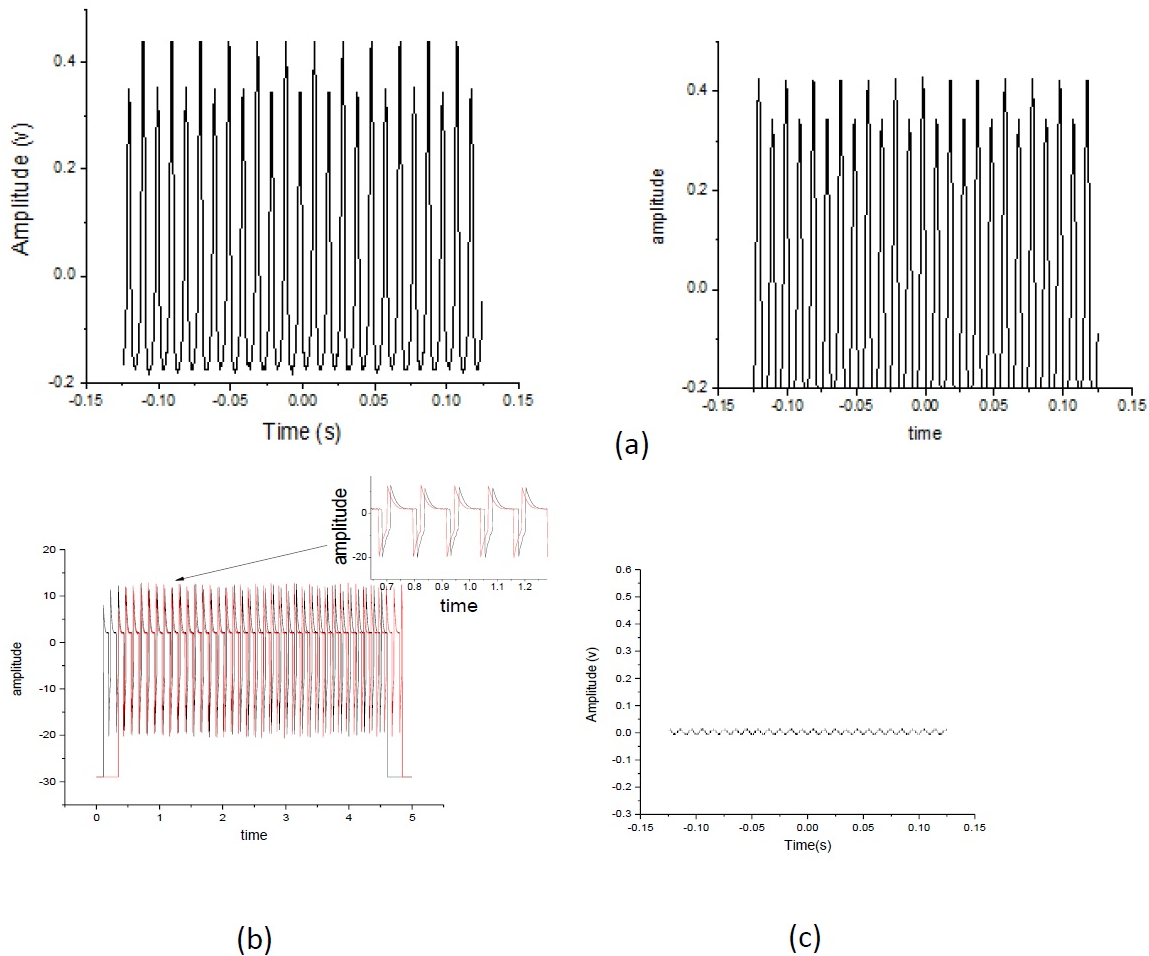


Figure 6: Synchronization of 2 opto-couplers. (a) time sequence of 1st opto-coupler and 2nd opto-coupler. (b) non-synchronization between 2 oscillators. (c) synchronization between 2 oscillators.

5. Experimental Results

In the sub-section, the results of synchronization regarding the 2 optoelectronic devices with AC-filtered non-linear optoelectronic feedback are shown. Various dynamical behaviors, such as chaotic as well as regular mixed mode oscillations, might be seen in each device (LED). The activity can be seen in a range of natural systems, including cardiac tissues, neural cells, and the chemical reactions. This method has also been known as (slow- fast systems). Two oscillators' outputs are fed into a variable gain operating amplifier, controlled by bias current, time series at the time t , and 1st and 2nd oscillators' feedback strengths. Those states have been depicted in fig.6a, where outputs of 2 oscillators have been coupled prior to occurrence of synchronization, as seen in fig.6b, and the non-synchronization between such 2 signals is plainly visible. The complete synchronization is displayed in Figure 6c.

Four LEDs were coupled for constructing a 2×2 network for optoelectronic oscillators; in such case, the bias current and feedback strength are utilized to feed all of the oscillators. Figure 7 shows the synchronization regarding the network with the feedback strength (\mathcal{E}) fixed and the bias current (δ) varied for each oscillator. Figure 7a shows the dynamical sequence, but Figure 7b shows no synchronization in the case when the g value is increased gradually. The entire synchronization of periodic mixed-mode oscillations was achieved by gradually increasing the spiking comes at the

same time sequences, as illustrated in Figure 7c.

In the system, the order degree has been identified using spatio-temporal distributions to quantify the rapid change. The phrase "spatio-temporal chaos" refers to irregular dynamical phenomena found in many of the spatially extended coupled chaotic systems. Also, the horizontal black bars show the intensities of optoelectronic devices, and the space-time symbolizes them. The largest spikes appear based on the previously-described process for network achieving synchronization, which indicates the fact that perturbation from 1st oscillator is in the propagation of the network, the entire array reaches last oscillator, and all peaks have a similar distribution of the times as can be seen from Fig. 8a. The oscillators are functioning separately, resulting in network non-synchronization. Figure 8b depicts the network's complete synchronization.

6. Conclusion

The experimental and numerical results of the unidirectional synchronization regarding LEDs networks have been reported. Spatio-Temporal distributions were evaluated across all interacting units to examine the synchronized state with regard to the time series and the spectra of oscillator outputs. The creation of a miniaturized LED network with numerous nodes that simulates a neural network is a significant benefit to technical applications.

Acknowledgments

F.F.A. would like to acknowledge the support of their colleagues from the physics dept., college of sciences, univ. of Baghdad for the assistance that they provided.

References

- [1] S.F. Abdalah, M. Ciszak, F. Marino, K. Al-Naimee, R. Meucci and F.T. Arecchi, *Optoelectronic Feedback in Semiconductor Light Sources: Optimization of Network Components for Synchronization*, Optoelectronic Devices and Properties, O. Sergiyenko (eds), IntechOpen, 2011.
- [2] S.F. Abdalah, M. Ciszak, F. Marino, K. Al-Naimee, R. Meucci and F.T. Arecchi, *Noise effects on excitable chaotic attractors in coupled light-emitting diodes*, IEEE Syst. J. 6 (2012) 558–563.
- [3] S. Abdalah, K. Al-Naimee, M. Ciszak, F. Marino, R. Meucci and F.T. Arecchi, *Chaos and mixed mode oscillations in optoelectronic networks*, Int. Rev. Phys. 7(3) (2013).
- [4] H. Fujisaka and T. Yamada, *Stability theory of synchronized motion in coupled-oscillator systems*, Prog. Theor. Phys. 69(1) (1983) 32–47.
- [5] D.M. Kane and K.A. Shore, *Unlocking Dynamical Diversity: Optical Feedback Effects On Semiconductor Lasers*, John Wiley & Sons, 2005.
- [6] M. Khan and S.N. Pal, *Synchronization of coupled chaotic systems using active control*, Int. J. Appl. Mech. Engin. 17(4) (2012) 1347–1353.
- [7] M. Khan, S.N. Pal and S. Poria, *Generalized anti-synchronization of different chaotic systems*, Int. J. Appl. Mech. Engin. 17(1) (2012) 83–99.
- [8] M.A. Khan and S. Poria, *Generalization synchronization of bidirectionally coupled Chaotic Systems*, Int. J. Appl. Math. Res. 1(3) (2012) 303–313.
- [9] H. Ghassan, K.A. Hubeatir and K.A.M. Al-Naimee, *Spiking control in semiconductor laser with Ac- coupled optoelectronic feedback*, Aust. J. Basic Appl. Sci. 9(33) (2015) 416–426.
- [10] Y. Liu, P. Davis and T. Aida, *Synchronized chaotic mode hopping in DBR lasers with delayed opto-electronic feedback*, IEEE J. Quantum Electron. 37 (2001) 337–352.
- [11] Y. Liu, P.C. de Oliveira, M.B. Danailov and J.R. Rios Leite, *Chaotic and periodic passive Q switching in coupled CO₂ lasers with a saturable absorber*, Phys. Rev. A. 50(4) (1994) 3464–3470.
- [12] R. Mainieri and J. Rehacek, *Projective synchronization in three-dimensional chaotic systems*, Phys. Rev. Lett. 82(15) (1999) 3042–3045.

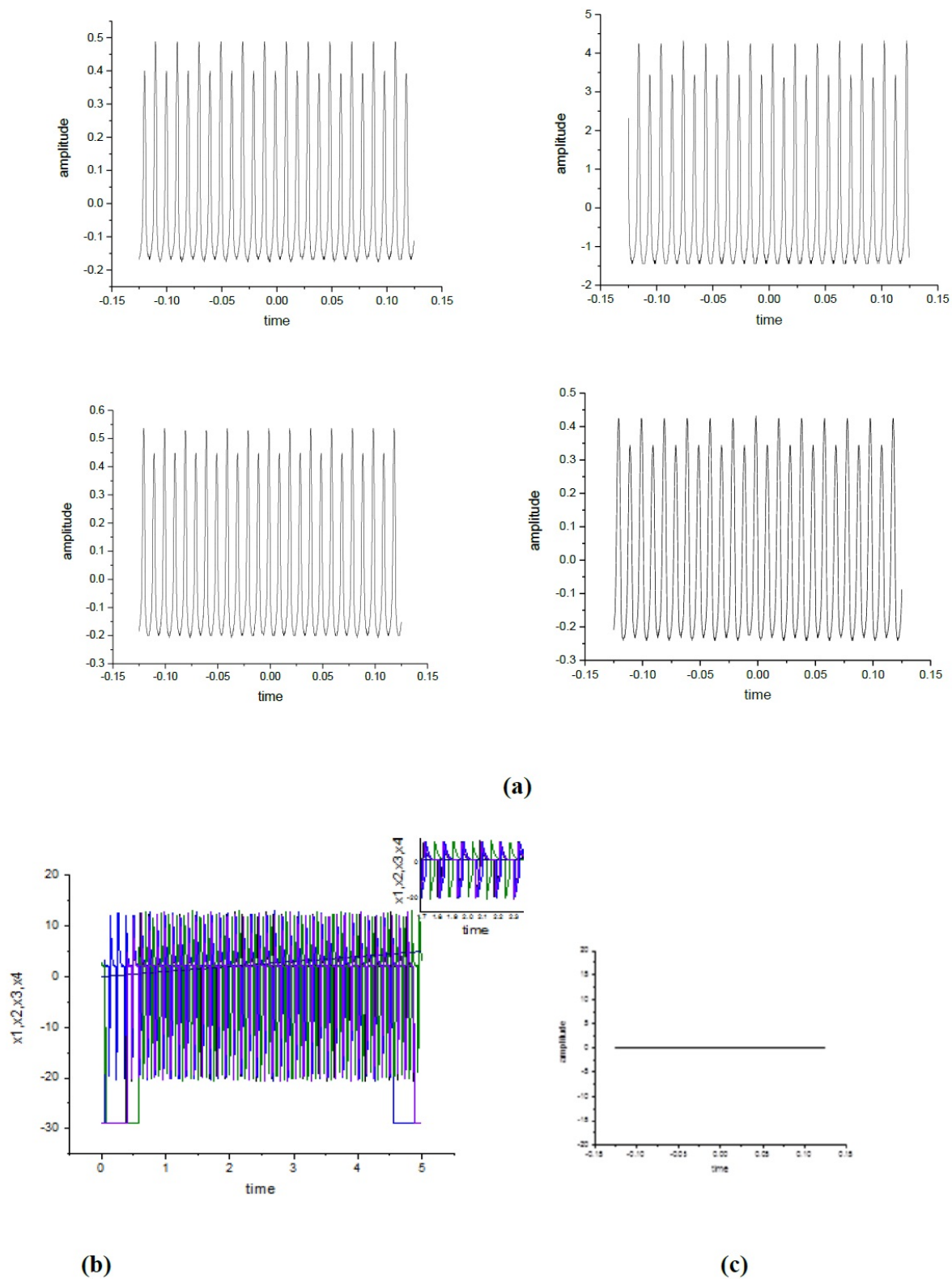


Figure 7: (a) The time series of 4 opto-couplers (b)non-synchronizations for 4 opto-couplers.(c) fully-synchronized.

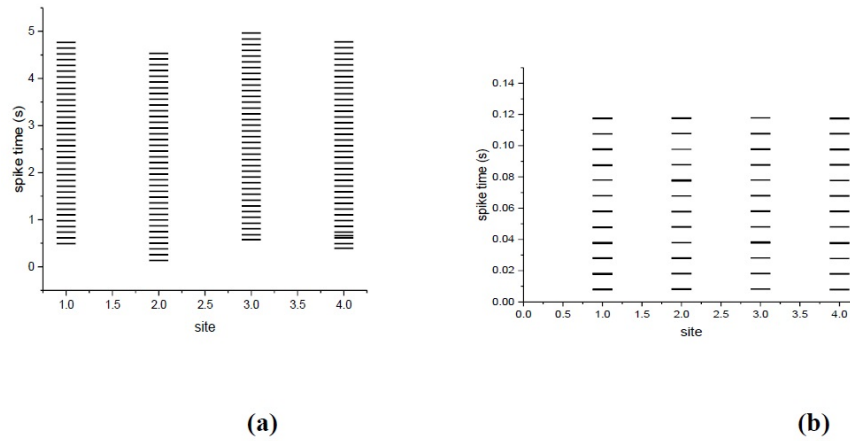


Figure 8: Spatiotemporal distribution for the experimental a) non-synchronization b) full-synchronization.

- [13] A.J. Obaid, *Critical Research on the Novel Progressive, JOKER an Opportunistic Routing Protocol Technology for Enhancing the Network Performance for Multimedia Communications*, In: R. Kumar, N.H. Quang, V.K. Solanki, M. Cardona and P.K. Pattnaik (eds), *Research in Intelligent and Computing in Engineering*, Adv. Intell. Sys. Comput., 1254, Springer, Singapore, 2021.
- [14] L.M. Pecora and T.L. Carroll, *Synchronization in chaotic systems*, Phys. Rev. Lett. 64(8) (1990) 821–824.
- [15] R. Regin, A.J. Obaid, A. Alenezi, F. Arslan, A.K. Gupta and K.H. Kadhim, *Node replacement based energy optimization using enhanced Salp swarm algorithm (Es2a) in wireless sensor networks*, J. Eng. Sci. Tech. 16(3) (2021) 2487–2501.
- [16] M.G. Rosenblum, A.S. Pikovsky and J. Kurths, *Phase synchronization of chaotic oscillators*, Phys. Rev. Lett. 76(11) (1996) 1804–1807.
- [17] M.G. Rosenblum, A.S. Pikovsky and J. Kurths, *From phase to lag synchronization in coupled chaotic oscillators*, Phys. Rev. Lett. 78(22) (1997) 4193–4196.
- [18] R. Roy and K.S. Thornburg, *Experimental synchronization of chaotic lasers*, Phys. Rev. Lett. 72 (1994) 2009–2012.
- [19] T. Sugawara, M. Tachikawa, T. Tsukamoto and T. Shimisu, *Observation of synchronization in laser chaos*, Phys. Rev. Lett. 72 (1994) 3502–3506.
- [20] A. Tarai(Poria), S. Poria and P. Chatterjee, *Synchronization of generalised linearly bidirectionally coupled unified chaotic system*, Chaos, Solitons Fractals 40(2) (2009) 885–892.
- [21] X.D. Wang, L.X. Tian and L.Q. Yu, *Linear feedback controlling and synchronization of eh Chen's chaotic system*, Int. J. Nonlinear Sci. 2 (2006) 43–49.
- [22] X. Wu and J. Hu, *Parameter identification and back steeping control of uncertain system*, Chaos, Solitons Fractals 18 (2003) 721–729.
- [23] T. Yamada and H. Fujisaka, *Stability theory of synchronized motion in coupled-oscillator Systems. II: The Mapping Approach*, Prog. Theor. Phys. 70(5) (1983) 1240–1248.